

Preparation of freestanding germanium nanocrystals by ultrasonic aerosol pyrolysis

Conrad R. Stoldt,^{a)} Michael A. Haag, and Brian A. Larsen

Department of Mechanical Engineering, University of Colorado, Boulder, Colorado 80309-0427, USA

(Received 16 June 2008; accepted 5 July 2008; published online 1 August 2008)

This letter reports a synthetic route adaptable for the continuous, large-scale production of germanium (Ge) nanocrystals for emerging electronic and optoelectronic applications. Using an ultrasonic aerosol pyrolysis approach, diamond cubic Ge nanocrystals with dense, spherical morphologies and sizes ranging from 3 to 14 nm are synthesized at 700 °C from an ultrasonically generated aerosol of tetrapropylgermane (TPG) precursor and toluene solvent. The ultimate crystal size demonstrates a near linear relationship within the range of TPG concentrations investigated, while the shape of the measured size distributions predicts multiple particle formation mechanisms during aerosol decomposition and condensation. © 2008 American Institute of Physics.

[DOI: [10.1063/1.2965471](https://doi.org/10.1063/1.2965471)]

In the last decade, significant research efforts have focused on the development of synthetic routes to freestanding semiconductor nanocrystals (NCs). Motivated by emerging applications in nonvolatile memory,¹ photosensors,^{2,3} solar conversion,^{4,5} and energy storage technologies,⁶ the size-tunable electronic and optical properties of NCs are utilized to achieve capabilities previously unattainable with bulk material systems. However, the proliferation of such next generation technologies hinges upon the development of synthetic processes capable of producing high quality materials in a readily scalable and continuous manner, as opposed to the conventional batch colloidal syntheses where throughput can be low and the quantity of toxic chemical reagents and waste can be high.⁷

While extensive work has focused on the development of group II-VI and III-V NCs, a far lesser body of work exists for the synthesis of freestanding group IV NCs such as Ge. The ongoing challenge with the nucleation and growth of these materials lies in the highly covalent character of their chemical bonds, where aggressive experimental conditions such as elevated temperatures are necessary to facilitate crystallization.⁸ As a consequence, only a handful of vapor phase routes have been described for the synthesis of freestanding Ge NCs, and include nonthermal plasma⁹ and high-pressure syntheses.^{10,11} These approaches are typically characterized by smooth, nearly spherical crystal morphologies, and have the potential for process scalability due to the continuous nature of the experimental design.

Ultrasonic aerosol pyrolysis (UAP) processes represent another route to the synthesis of ultrafine particles, where submicron materials are produced by the ultrasonic nebulization of one or more molecular precursors followed by their thermal decomposition and condensation in a flow tube to form freestanding particles. Variations of this vapor phase process have been applied to the synthesis of metal oxides¹²⁻¹⁴ and group II-VI NCs.¹⁵ Generally, particle formation by this process occurs by two possible mechanisms: intradroplet reaction or gas-to-particle conversion.^{13,14} In the intradroplet reaction mechanism, each droplet converts into a

single solid particle via the one-droplet-to-one-particle (ODOP) conversion process. The gas-to-particle conversion mechanism occurs when a volatile particle precursor is transported across the particle-gas interface, where it either nucleates new particles or condenses on previously formed particles. The observation of bimodal size distributions in particles resulting from aerosol decomposition is previously attributed to process conditions where both formation mechanisms are operative.¹⁴ Bimodality is also attributed to aerosol droplet coagulation prior to particle formation, primarily resulting from aerosols with high initial droplet concentrations.¹⁵ Overall, the ultrasonic aerosol decomposition approach is industrially important, as the process is low cost and easily scaled for continuous and high throughput production.

In this letter, we utilize UAP to prepare size tuned Ge NCs, a group IV material that is of significant technological interest due in part to quantum confinement effects arising from very small particle diameters.¹⁶⁻¹⁸ The UAP apparatus consists of a vertically oriented, 1 in. diameter quartz tube in a three-zone tube furnace. The first two zones of the furnace were held at 700 °C for the thermal decomposition of Ge precursor and condensation of the Ge NCs, followed by the third zone held at 350 °C for gradual cooling of the Ge product. The resulting Ge NCs were captured as a colloid in a bubbler containing trichloroethylene (TCE). The Ge NC precursor solution, comprised of a mixture of tetrapropylgermane (TPG) and toluene, was delivered to the 1.7 MHz ultrasonic transducer by a syringe pump. Upon nebulization, the precursor aerosol comprised of between 0.025% and 0.065% vol./vol. TPG in toluene was transported by ultra-high purity Ar carrier gas to the tube furnace. The Reynolds number for the carrier gas in the hot zone was calculated to be ~20, which is well within the laminar flow regime.

At fixed Ar flow rate and furnace temperature, the mean size of the Ge NCs can be tuned via variation of the TPG:toluene in the precursor solution, which in turn adjusts the amount of TPG per aerosol droplet. Figure 1 shows representative transmission electron microscopy (TEM) images of the Ge NCs produced by the UAP process. The Ge NCs have a near spherical morphology that is characteristic of particles synthesized by aerosol decomposition

^{a)}Electronic mail: stoldt@colorado.edu.

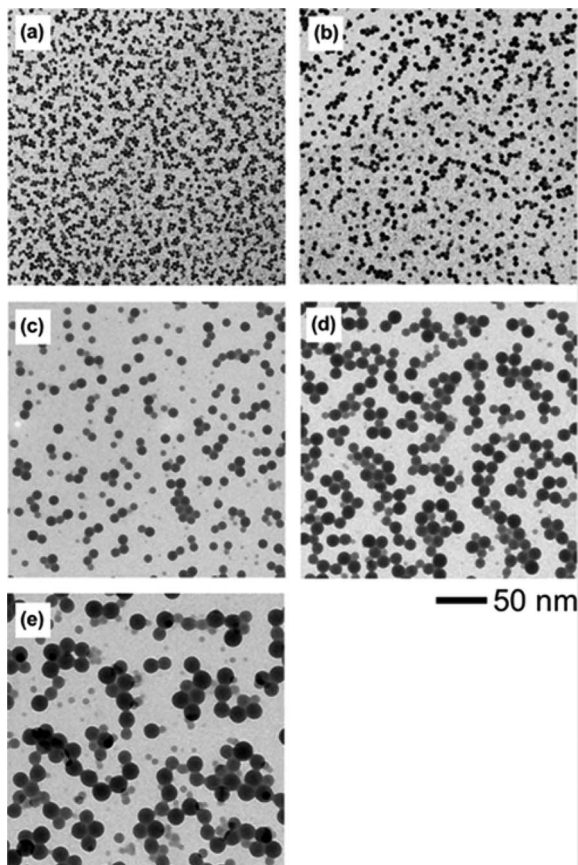


FIG. 1. Representative TEM images of Ge NCs with mean diameters of (a) 3.1 ± 0.4 nm, (b) 4.0 ± 0.6 nm, (c) 7.0 ± 1.6 nm, (d) 9.7 ± 2.0 nm, and (e) 11.1 ± 3.6 nm synthesized at 700°C from 25, 35, 45, 55, and $65 \mu\text{l}$ of TPG per 100 ml of toluene, respectively. The standard deviation in NC diameter (measured from over 1000 particles per TEM image) ranges from about 10% to 30% and increases with TPG volume per aerosol droplet.

processes.^{12–14} In addition, the NCs are not agglomerated, but instead show a uniform distribution with easily defined boundaries after the drop-casting process from TCE for TEM imaging. The NC mean diameter is observed to increase from about 3.1 to 11.1 nm as the volume of TPG in the precursor solution is increased from 25 to $65 \mu\text{l}$, respectively. Similarly, the standard deviations (measured from over 500 particles per TEM image) range from about 10% to 30% and increase with NC size.

High-resolution TEM (HRTEM) and x-ray diffraction (XRD) confirmed that the Ge product was crystalline with diamond cubic structure. The Ge NCs exhibited single-crystal domains over the range of sizes imaged, as shown in Fig. 2(a), where representative HRTEM images of particles with approximate diameters of 13 and 10 nm are shown. The measured d spacings of about 3.2 and 2.0 \AA from the resolved fringes correspond to the Ge $\{111\}$ and $\{220\}$ planes. The characteristic XRD pattern shown in Fig. 2(b) identifies diamond cubic structure with reflections that match the expected $\{111\}$, $\{220\}$, and $\{311\}$ diffraction peaks of bulk Ge, as previously observed in NCs prepared by both gas^{9–11} and liquid phase syntheses.^{19–21} As compared to traditional liquid syntheses where the particles appear coarse with inconsistent morphologies, Ge NCs produced by UAP are nearly spherical with well-defined, smooth edges. The irregular nature of particles produced by liquid phase processes may result from uncontrolled ripening during the stirred reaction²² or insuffi-

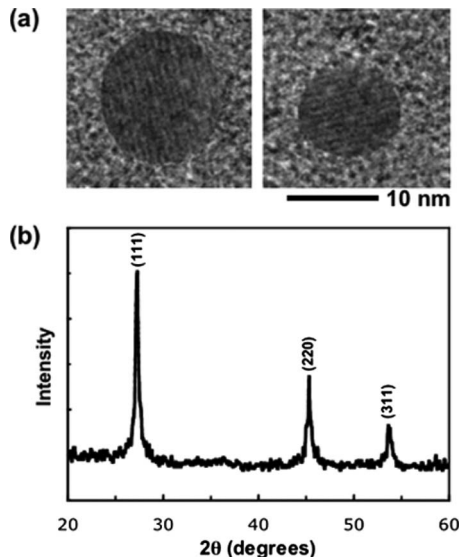


FIG. 2. (a) HRTEM images of ~ 13 and 10 nm Ge NCs synthesized from 55 and $65 \mu\text{l}$ of TPG per 100 ml of toluene, respectively. HRTEM images show lattice fringes for most of the NCs analyzed. The measured d spacings of ~ 3.2 and 2.0 \AA correspond to the $\{111\}$ and $\{220\}$ planes of diamond cubic Ge. (b) Powder XRD spectrum of a representative Ge NC preparation shows the characteristic $\{111\}$, $\{220\}$, and $\{311\}$ diffraction peaks for diamond cubic Ge.

cient temperatures for atomic restructuring during growth.⁸

The effect of TPG volume in the precursor solution on the resulting NC mean diameter is quantitatively summarized in Fig. 3(a), where a near linear relationship ($R^2=0.96$) is observed for NC diameters approaching 14 nm prepared by UAP. In order to better understand the observed particle size and size distribution with increasing TPG precursor volume, the resulting data was analyzed using the ODOP principle. In general, the causal relationship between the mean size and size distribution of precursor containing aerosol droplets and the resulting thermally processed solid particles is not well understood.¹³ Parameters that influence the droplet and final product mean size and size distribution include the droplet

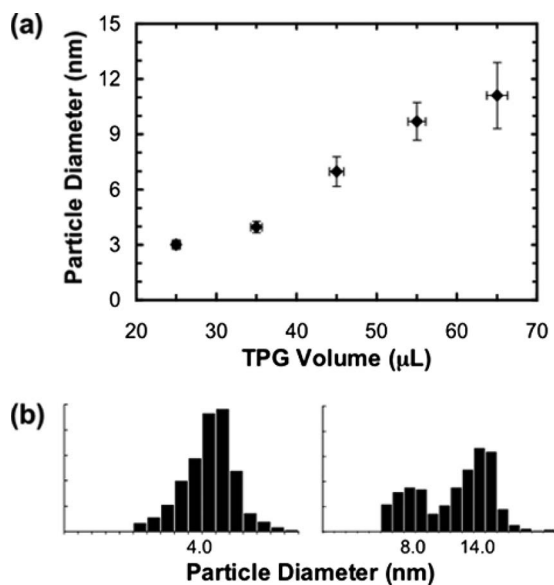


FIG. 3. (a) Ge NC mean diameter plotted as a function of Ge precursor volume in microliters of TPG per 100 ml of toluene. (b) Size distributions for Ge NCs with mean diameters of 4.0 and 11.1 nm.

temperature, the ultrasonic nebulization rate, the carrier gas flow rate, interactions with the reactor walls, and the solution precursor concentration.

The mean droplet size produced by an ultrasonic transducer can be estimated using Lang's equation.¹³ Since each aerosol droplet produced by our transducer is primarily toluene solvent (>99.9% by volume), we estimate the mean droplet diameter to be $\sim 2.2 \mu\text{m}$, although it is previously noted that the solute physicochemical properties can shift the mean droplet size downward.¹³ In the ODOP mechanism, the relationship between the mean droplet size and the corresponding mean particle diameter is dependent on the precursor solution mass fraction and NC density. Here, the ODOP mechanism predicts Ge NC diameters ranging from ~ 52 to 70 nm utilizing the TPG quantities shown in Fig. 3(a) and an initial aerosol droplet size of $2.2 \mu\text{m}$. These size estimates are significantly larger than the mean particle diameters produced in this study, but our results can be understood if additional factors beyond the ODOP mechanism are operative in determining the final NC product.

Further analysis of the TEM images in Fig. 1 shows the presence of NCs having a size less than the average, which is readily resolved in Figs. 1(c)–1(e). In Fig. 3(b), the size distributions of NCs with mean diameters of 4.0 and 11.1 nm are shown. Both distributions are skewed left, with the 11.1 nm diameter sample in Fig. 3(b) exhibiting a distinct bimodal distribution with modes near 8 and 14 nm . With an initial aerosol droplet size of $2.2 \mu\text{m}$, our results indicate that the gas-to-particle conversion mechanism for particle formation also occurs under the experimental conditions used here, thus resulting in an overall mean NC size smaller than predicted by the ODOP mechanism alone and the observed bimodal or skewed left NC size distributions. In Fig. 3(b), the secondary mode is less than the mean particle diameter of 11.1 nm , which is consistent with reported results for particle formation by both gas-to-particle conversion and the ODOP mechanism.¹⁴ Furthermore, the absence of a mode greater than the mean particle diameter indicates that droplet coagulation before pyrolysis is not significant.¹³

In summary, UAP of TPG at $700 \text{ }^\circ\text{C}$ yielded diamond cubic Ge NCs with average sizes between ~ 3 and 11 nm . The range of NC sizes prepared in this study are of significant utility to emerging electronic and optoelectronic tech-

nologies where quantum size effects are expected to prescribe the material properties.

The authors acknowledge Dennis Eberl of the USGS and Barbara Hughes of NREL for their assistance in acquiring XRD and HRTEM data, respectively. The University of Colorado at Boulder and DARPA are also acknowledged for their support of this research work.

- ¹T. Feng, H. Yu, M. Dicken, J. R. Heath, and H. A. Atwater, *Appl. Phys. Lett.* **86**, 033103 (2005).
- ²G. Konstantatos, I. Howard, A. Fischer, S. Hoogland, J. Clifford, E. Klem, L. Levina, and E. H. Sargent, *Nature (London)* **442**, 180 (2006).
- ³W.-J. Chiang, C. Y. Chen, C. J. Lin, Y. C. King, A. T. Cho, C. T. Peng, C. W. Chao, K. C. Lin, and F. Y. Gan, *Appl. Phys. Lett.* **91**, 051120 (2007).
- ⁴I. Gur, N. A. Fromer, M. L. Geier, and A. P. Alivisatos, *Science* **310**, 462 (2005).
- ⁵A. Maria, P. W. Cyr, E. J. D. Klem, L. Levina, and E. H. Sargent, *Appl. Phys. Lett.* **87**, 213112 (2005).
- ⁶H. Li, X. Huang, L. Chen, Z. Wu, and Y. Liang, *Electrochem. Solid-State Lett.* **2**, 547 (1999).
- ⁷C. J. Murphy, *J. Mater. Chem.* **18**, 2173 (2008).
- ⁸J. R. Heath and J. J. Shiang, *Chem. Soc. Rev.* **27**, 65 (1998).
- ⁹R. Gresback, Z. Holman, and U. Kortshagen, *Appl. Phys. Lett.* **91**, 093119 (2007).
- ¹⁰X. Lu, K. J. Ziegler, A. Ghezelbash, K. P. Johnston, and B. A. Korgel, *Nano Lett.* **4**, 969 (2004).
- ¹¹D. Gerion, N. Zaitseva, C. Saw, M. F. Casula, S. Fakra, T. Van Buuren, and G. Galli, *Nano Lett.* **4**, 597 (2004).
- ¹²B. Xia, I. W. Lenggoro, and K. Okuyama, *Adv. Mater. (Weinheim, Ger.)* **13**, 1579 (2001).
- ¹³W.-N. Wang, A. Purwanto, I. W. Lenggoro, K. Okuyama, H. Chang, and H. D. Jang, *Ind. Eng. Chem. Res.* **47**, 1650 (2008).
- ¹⁴C. Y. Chen, T. K. Tseng, S. C. Tsai, C. K. Lin, and H. M. Lin, *Ceram. Int.* **34**, 409 (2008).
- ¹⁵Y. T. Didenko and K. S. Suslick, *J. Am. Chem. Soc.* **127**, 12196 (2005).
- ¹⁶Y. M. Niquet, G. Allan, C. Delerue, and M. Lannoo, *Appl. Phys. Lett.* **77**, 1182 (2000).
- ¹⁷L. Dal Negro, M. Cazzanelli, L. Pavesi, S. Ossicini, D. Pacifici, G. Franzo, F. Priolo, and F. Iacona, *Appl. Phys. Lett.* **82**, 4636 (2003).
- ¹⁸M. C. Beard, K. P. Knutsen, P. Yu, J. M. Luther, Q. Song, W. K. Metzger, R. J. Ellingson, and A. J. Nozik, *Nano Lett.* **7**, 2506 (2007).
- ¹⁹X. Lu, B. A. Korgel, and K. P. Johnston, *Chem. Mater.* **17**, 6479 (2005).
- ²⁰H. Gerung, S. D. Bunge, T. J. Boyle, C. J. Brinker, and S. M. Han, *Chem. Commun. (Cambridge)* **2005**, 1914.
- ²¹H. P. Wu, M. Y. Ge, C. W. Yao, Y. W. Wang, Y. W. Zeng, L. N. Wang, G. Q. Zhang, and J. Z. Jiang, *Nanotechnology* **17**, 5339 (2006).
- ²²A. J. Barker, B. Cage, S. Russek, and C. R. Stoldt, *J. Appl. Phys.* **98**, 063528 (2005).

Applied Physics Letters is copyrighted by the American Institute of Physics (AIP). Redistribution of journal material is subject to the AIP online journal license and/or AIP copyright. For more information, see <http://ojps.aip.org/aplo/aplcr.jsp>